ARTICLE

Elucidating structural and compositional changes in plant tissues and single cells by Raman spectroscopic imaging

Batirtze Prats Mateu,[a] Barbara Stefke,[a] Marie-Theres Hauser[b] and Notburga Gierlinger[a,c,d]

[a]Department of Materials Sciences and Process Engineering, BOKU-University of Natural Resources and Life Sciences, Vienna, Austria. E-mail: burgi.gierlinger@boku.ac.at

[b]Department of Applied Genetics and Cell Biology, BOKU-University of Natural Resources and Life Sciences, Vienna, Austria

[c]Institute for Building Materials, ETH Zurich, Zurich 8093, Switzerland

[d]Applied Wood Research Laboratory, Empa—Swiss Federal Laboratories for Material Testing and Research, 8600 Dübendorf, Switzerland

Introduction

Plants represent the most abundant source of terrestrial biomass and renewable energy and are of practical importance for human and animal nutrition as well as a source of natural fibres for textiles, materials and paper products. The understanding of plant cells is thus of high interest for optimised utilisation of plants in traditional and new applications and also from the biomimetic view, as nature has evolved a variety of plant cell walls differing in properties and functionalities and adapted to different habitats and environments.

In all plants, the cell walls make up the major part of the biomass and are based on crystals of cellulose forming microfibrils, which are embedded in different matrix polymers. Two types of plant cell walls can be distinguished: primary walls are deposited during cell growth, and secondary cell walls after cell growth has ceased. Primary cell walls need to be both mechanically stable and sufficiently extensible to permit cell expansion while avoiding the rupture of cells under their turgour pressure. This is achieved by rather stiff cellulose microfibrils embedded in a water-rich matrix of hemicelluloses, pectins and proteins. In contrast,

secondary cell walls are often made "waterproof" and more stable and resistant by their impregnation with lignins, an aromatic polymer composed of phenylpropane units. Moreover, the secondary plant cell wall of wood is composed of sub-layers (S1, S2 and S3), differing in chemical composition and the alignment of the cellulose microfibrils with respect to the fibre axis (cellulose microfibril angle, MFA). To glue adjacent cells together to form functional

tissues matrix polymers are deposited between the cells in the cell corner (CC) and compound middle lamella (CML) ensuring the adhesion of a cell to its neighbours. All plant parts exposed to the atmosphere are coated with layers of lipid materials (cutin, suberin and waxes) that reduce water loss and help block the entry of pathogenic fungi and bacteria. The chemical composition and structure of the cells and their arrangement show significant inter- and

*Arabidopsis thaliana*   *Ailanthus altissima*

ARTICLE
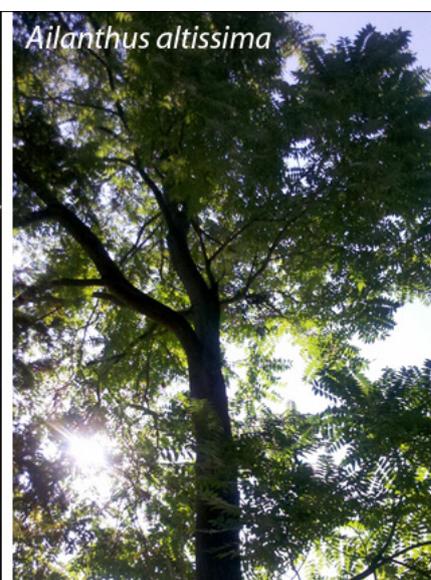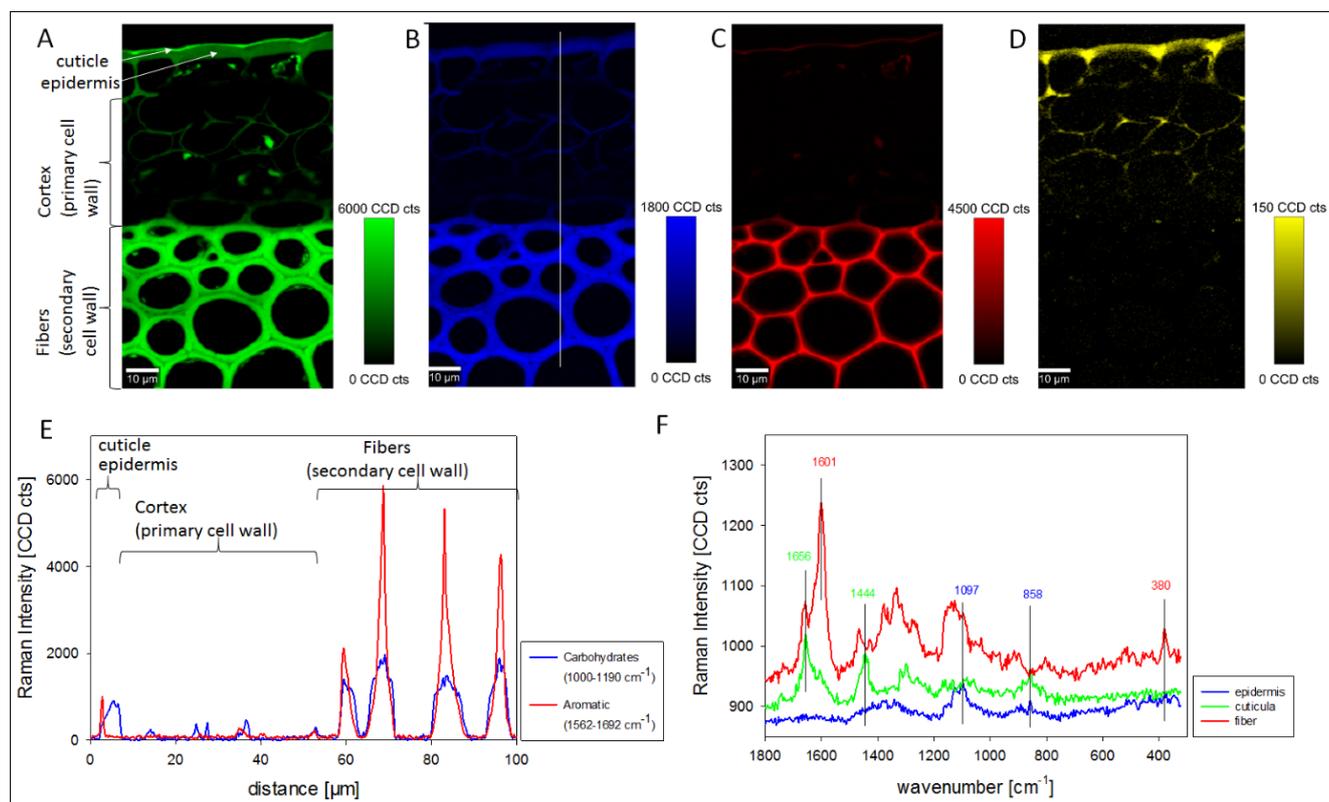
Figure 1. Raman images of a transverse section through the stem of *Arabidopsis thaliana* calculated by integration over the wavenumber range of 2845–3044 cm^{-1} (A, CH stretching region), 1000–1190 cm^{-1} (B, mainly carbohydrates[7]), 1562–1692 cm^{-1} (C, aromatic ring and C=O stretch of lignin[7]) and 840–880 cm^{-1} (D, α-1–4-glycosidic bond in pectin[8]). Highlighted areas correspond to the maximum intensity of the component in the section. Chemical profile (E) of an imaginary cross-section (white line in 1B) with special attention to the intensity of carbohydrates (blue) and the aromatic compounds (red). Exemplary single spectra extracted from the epidermis (blue), the cuticle (green) and from a fibre (red) are plotted in (F). (Experimental: 532 nm excitation, 100× oil immersion objective NA = 1.4, scan area: 60 × 100 µm, Pixels: 180 × 300, integration time: 0.09 s.)

intra-species variability and determine the different tissue and surface properties.[1,2]

Most traditional chemical analyses of plant tissues are destructive, since they require disintegration. However, the functional characteristics of plant tissues do not solely depend on their chemical composition *per se*, but also on the distribution of the different components in the context of their micro- and nano-structure and their interaction. During recent years confocal Raman micros-copy has evolved as an important tool in plant cell wall research, as changes in the molecular composition can be observed and imaged with a diffraction limited spatial resolution (~300 nm) in the native plant tissues.[3–5] Sample preparation methods for plant cell walls, measurement parameters as well as spectral data analysis approaches are described in detail elsewhere.[6] In this article the potential of the Raman spec-

troscopic imaging approach is shown for two examples: 1) visualising changes in the chemical composition within the cross-section of a stem of the model plant *Arabidopsis thaliana* by simply integrating marker bands of plant cell wall polymers, and 2) revealing fine details of the wooden tissue of *Ailanthus altissima* by vertex component analysis (VCA), a multivariate approach.

Imaging different cell types in the stem of *Arabidopsis thaliana*

On a microtomed cross-section through the stem of *Arabidopsis thaliana* (a small flowering plant widely used as a model organism in plant biology) an area of interest of 60 × 100 µm was selected and Raman spectra acquired every 0.3 µm with an integration time of 0.09 s. Based on the 54,000 spec-tra, Raman images were calculated by

integrating different bands attributed to the functional groups of plant cell wall polymers (see Figures 1 A–D). By inte-grating the stretching vibration of the CH groups, which are present in all plant molecules, all structures are visu-alised (Figure 1A). The outer surface, the cuticle, is highlighted as well as the epidermis, primary cell walls in the cortex, secondary cell walls in the fibres and also some deposits within the cell lumina. Integrating the region characteristic for carbohydrates (cellu-lose, hemicellulose, pectin) most of the cell walls in the epidermis, cortex and fibres are highlighted (Figure 1B), whereas by integrating the lignin marker band around 1601 cm^{-1} the intensity is mainly restricted to the fibres and within the fibres enriched in the cell corners (Figure 1C). In contrast the pectin marker band (856 cm^{-1}) shows highest intensity in the epidermis and progres-

sively decreases along the cortex, where it is mainly restricted to the cell corners (Figure 1D). The change in intensities along different tissue types and cells can be shown in more detail by defining a line of interest (vertical white line shown in Figure 1B) and plotting the change of the integrated area along this line (Figure 1E). It is clearly visible that carbohydrates show a high intensity in the epidermis and in the fibres, whereas lignin shows an increase at the outer cuticle, absence in the primary cell wall of the cortex and the highest intensity in the fibres. The lignin and carbohydrate profiles within the fibres differ, showing an accumulation of lignin in the middle of two neighbouring cell walls (Figure 1E). These simple image and plot calculations based on the integrals of the marker bands of plant cell wall polymers give a rapid overview on the overall structure (Figures 1 A–B) and the changes in chemistry at the micro level: 1) a high amount of pectin in the epidermis and primary cell walls in contrast to the lignified fibres (Figures 1 C–D), and 2) both aforementioned matrix polymers are deposited within the cell walls, but in highest amounts in cell corners and between the cells for gluing them together (Figures 1 C–E).

Associated with each pixel in the Raman image there is a spectrum representing a molecular fingerprint at every mapped position. Thus detailed insights on the molecular composition at every point or for every tissue type can be gained by extracting a single spectrum (one pixel, Figure 1F) or average spectra,[3] respectively. Extracting single spectra within the different cells demonstrates that the chemistry of the cuticle (Figure 1F, green spectrum) differs clearly from the cell walls (red and blue spectra). As far as the cuticle is concerned: the two characteristic bands in the cuticle spectrum at 1650 cm^{-1} and around 1440 cm^{-1} (Figure 1F, green spectrum) can be assigned to the C=C stretch indicating chain unsaturation in fatty acids and the –CH$_2$ bending of saturated CH$_2$ bonds, respectively,[9] as the cuticle is reported to consist mainly of lipids such as triterpenoids and very long cuticular wax components (alkanes, alcohols and

fatty acids).[10] This spectral analysis clarifies that the higher intensity of the "lignin integration" in the cuticle (Figures 1 C, E) does not derive from lignin bands, but are due to the band at 1650 cm^{-1} attributed to unsaturated fatty acids. In contrast to microscopic staining or fluorescence images, Raman spectroscopic images have thus the potential to evaluate the underlying spectra and thereby to avoid misinterpretation of results and gain more detailed insights into the molecular composition. The spectrum of the epidermis shows peaks at 858 cm^{-1} and 1097 cm^{-1} (Figure 1F, blue spectrum), which confirm a high content of pectin together with other carbohydrates (cellulose). The spectrum deriving from the secondary cell wall of the fibre shows the highest intensity (Figure 1F, red spectrum), as these have the thickest and densest cell walls. These secondary cell

wall spectra clearly show contributions of cellulose (380 cm^{-1}, 1097 cm^{-1}) and lignin (1601 cm^{-1} and 1660 cm^{-1}), which also gives rise to a higher fluorescence background (Figure 1F, red spectrum).

Changes within wooden cell walls of *Ailanthus altissima*

Ailanthus altissima, a fast growing deciduous hardwood tree native to China and Taiwan, has become an invasive species in Europe. Its wooden cell walls represent lignified secondary cell walls and its Raman spectra are composed of many overlapping bands deriving from cellulose, hemicelluloses and lignin. For such spectral data sets multivariate analysis methods [e.g. cluster analysis or vertex component analysis (VCA)], which do not only take one marker band into account but the whole wavenumber
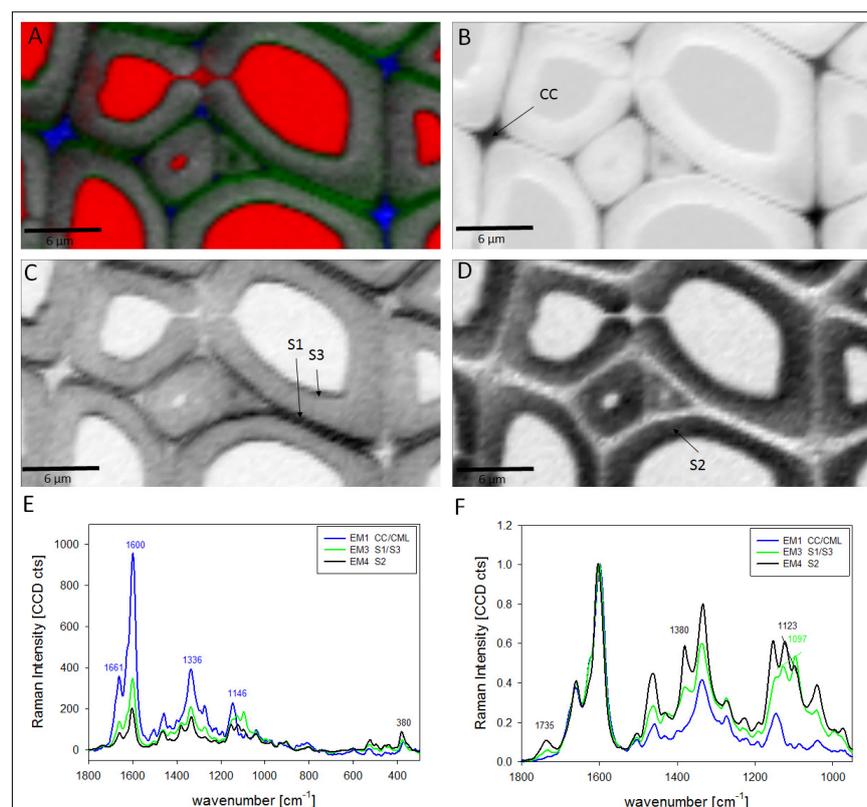

Figure 2. Raman images of *Ailanthus altissima* wood cross-section based on vertex component analysis (VCA) with four end members (EMs) using the region from 1800 cm^{-1} to 300 cm^{-1}: combination image of all four EMs (A) and abundance map of EM 1 corresponding to the cell corner (CC) and compound middle lamella (CML) (B), EM 3 reflecting the S1/S3 cell wall layers (C) and EM 4 highlighting the S2 layer (D). The EM spectra are summarised without spectral treatment (E) and after baseline correction and normalisation on the aromatic stretching vibration at 1600 cm^{-1} (F). (Experimental: 532 nm excitation, 100× oil immersion objective, scan area: 33 × 18 µm, Pixels: 99 × 54, integration time: 0.09 s.)

ARTICLE

range, are often advantageous.[11] Using VCA a spectral data set can be decomposed by extracting pure components, so called endmembers (EMs).[12] By this approach different anatomical structures and cell wall layers can be visualised and the underlying molecular structure can be derived based on the EM spectra.[13] Applied to wooden tissue samples of *Ailanthus altissima,* VCA revealed that the cell corners (Figure 2A, blue colour) are clearly different from the secondary cell wall (grey colour), in which additionally a small layer (green colour) was separated. The cell corners are represented by the first EM (Figure 2B) and characterised by almost pure lignin composition as can be derived from the EM spectrum (Figure 2E, F blue spectrum) showing the typical lignin bands at $1661\,cm^{-1}$, $1600\,cm^{-1}$, $1336\,cm^{-1}$ and $1146\,cm^{-1}$. The second EM represents the cell lumen (Figure 2A, red colour), the third and fourth EMs the secondary cell wall (Figure 2A, grey and green colours). The EM spectra of the secondary cell wall show beside the lignin bands additional peaks at $1736\,cm^{-1}$ deriving from hemicelluloses and $1380\,cm^{-1}$, $1123\,cm^{-1}$, $1097\,cm^{-1}$ and $380\,cm^{-1}$ due to cellulose (Figure 2 E–F, green and black spectra). Comparing in more detail the shape of the lignin region after normalisation changes in lignin composition between cell corner and secondary cell wall can be seen (Figure 2F).[12] The third EM represents mainly the thin outer layer of the secondary cell wall (S1) and the layer towards the lumen (S3) (Figure 2C). These thin layers differ from the rest of the thick secondary cell wall (S2, Figure 2D) by having higher lignin content and different cellulose orientation (Figures 2 E–F). The fact that the cellulose microfibrils are oriented with a higher angle with respect to the fibre axis in S1 and S3 can be derived from the change of the height of the cellulose sensitive band at $1097\,cm^{-1}$ in relation to that of the $1122\,cm^{-1}$ band (Figure 2F).[14] In this example it is again shown that VCA is a very promising method in hyperspectral image analysis due to the easy and simple way one can unravel common features in a region of inter-est and reveal changes in the molecular structure.[13]

Outlook

While most analytical techniques are destructive, Raman spectroscopic imaging represents one of the best ways to unravel the molecular structure in the native environment of plant tissues. Changes in chemical composition can be located between and within different cells with a spatial resolution of about ~300 nm. The examples shown here are just two out of many possibilities for Raman spectroscopic imaging and analysis. Although univariate spectral analysis gives a fast and good quality picture of the chemical and anatomical composition, multivariate analyses are the most promising methods in unravelling more fine details even when bands are overlapping. In the future, multivariate hyperspectral image analyses combined with reference Raman spectroscopy measurements and spectral databases of different plant components and plant species and their different tissues will help us to gain a better understanding of the plant spectral signatures and unravel more information out of the molecular fingerprints at every mapped position. Also small particles or deposits within the cell can be analysed and plant growth processes followed step by step, e.g. by following the incorporation of the lignin polymer from the cambial cells to the final secondary cell wall. The method is not restricted to one plant part, but can be applied from the root over the stem to the leaves and will help to gain a more comprehensive picture of plant tissues including important cell and organ surfaces. Additionally, reactions could be tracked in line with environmental changes and adaptations or changes due to genetic modifications.

Acknowledgements

References

1. R.A. Burton, M.J. Gidley and G.B. Fincher, "Heterogeneity in the chemistry, structure and function of plant cell walls", *Nature Chem. Biol.* **6,** 724–732 (2010). doi: http://dx.doi.org/10.1038/nchembio.439

2. D. Fengel and G. Wegener, *Wood: Chemistry, Ultrastructure, Reactions.* Walter de Gruyter & Co., Berlin (1989).

3. N. Gierlinger and M. Schwanninger, "Chemical imaging of poplar wood cell walls by confocal Raman microscopy", *Plant Physiol.* **140,** 1246–1254 (2006). doi: http://dx.doi.org/10.1104/pp.105.066993

4. N. Gierlinger and M. Schwanninger, "The potential of Raman microscopy and Raman imaging in plant research", *Spectrosc.–Int. J.* **21,** 69–89 (2007).

5. U. Agarwal, "Raman imaging to investigate ultrastructure and composition of plant cell walls: distribution of lignin and cellulose in black spruce wood (*Picea mariana*)", *Planta* **224,** 1141–1153 (2006). doi: http://dx.doi.org/10.1007/s00425-006-0295-z

6. N. Gierlinger, T. Keplinger and M. Harrington, "Imaging of plant cell walls by confocal Raman microscopy", *Nature Protoc.* **7,** 1694–1708 (2012). doi: http://dx.doi.org/10.1038/nprot.2012.092

7. U.P. Agarwal and S.A. Ralph, "FT-Raman spectroscopy of wood: identifying contributions of lignin and carbohydrate polymers in the spectrum of black spruce (*Picea mariana*)" *Appl. Spectrosc.* **51,** 1648–1655 (1997). doi: http://dx.doi.org/10.1366/0003702971939316

8. A. Synytsya, J. Copikova, P. Matejka and V. Machovic, "Fourier transform Raman and infrared spectroscopy of pectins", *Carbohyd. Polym.* **54,** 97–106 (2003). doi: http://dx.doi.org/10.1016/S0144-8617(03)00158-9

9. M.M.L. Yu, H.G. Schulze, R. Jetter, M.W. Blades and R.F.B. Turner, "Raman microspectroscopic analysis of triterpenoids found in plant cuticles", *Appl. Spectrosc.* **61,** 32–37 (2007). doi: http://dx.doi.org/10.1366/0003702077979701352

10. J.A. Heredia-Guerrero, J.J. Benítez, E. Domínguez, I.S. Bayer, R. Cingolani, A. Athanassiou and A. Heredia, "Infrared and Raman spectroscopic features of plant cuticles: a review", *Front. Plant Sci.* **5,** 305 (2014). doi: http://dx.doi.org/10.3389/fpls.2014.00305

11. A. de Juan, M. Maeder, T. Hancewicz, L. Duponchel and R. Tauler, "Chemometric tools for image analysis", in *Infrared and Raman Spectroscopic Imaging*, Ed by R. Salzer and H.W. Siesler. Wiley-VCH, Weinheim, pp. 65–108 (2009). doi: http://dx.doi.org/10.1002/9783527628230.ch2

12. J.M.P. Nascimento and J.M.B. Dias, "Vertex component analysis: A fast algorithm to unmix hyperspectral data" *IEEE Trans. Geosci. Remote Sens.* **43,** 898–910 (2005). doi: http://dx.doi.org/10.1109/TGRS.2005.844293

13. N. Gierlinger, "Revealing changes in molecular composition of plant cell walls on the micron-level by Raman mapping and vertex component analysis (VCA)", *Front. Plant Sci.* **5,** 306 (2014). doi: http://dx.doi.org/10.3389/fpls.2014.00306

14. N. Gierlinger, S. Luss, C. König, J. Konnerth, M. Eder and P. Fratzl, "Cellulose microfibril orientation of *Picea abies* and its variability at the micron-level determined by Raman imaging", *J. Exp. Bot.* **61,** 587–595 (2010). doi: http://dx.doi.org/10.1093/jxb/erp325